

Received April 28, 2021, accepted May 13, 2021, date of publication May 17, 2021, date of current version May 26, 2021.

Digital Object Identifier 10.1109/ACCESS.2021.3081349

# The Noise Attenuation and Stochastic Clutter Removal of Ground Penetrating Radar Based on the K-SVD Dictionary Learning

DESHAN FENG<sup>1,2</sup>, SHUO LIU<sup>1,2</sup>, JUN YANG<sup>3</sup>, XIANGYU WANG<sup>1,2</sup>, AND XUN WANG<sup>1,2</sup>

<sup>1</sup>School of Geosciences and Info-Physics, Central South University, Changsha 410083, China

<sup>2</sup>Key Laboratory of Metallogenic Prediction of Nonferrous Metals and Geological Environment Monitoring, Ministry of Education, Changsha 410083, China

<sup>3</sup>Guangzhou Municipal Engineering Design and Research Institute Company Ltd., Guangzhou 510000, China

Corresponding author: Xiangyu Wang (nephilim.csu@gmail.com)

This work was supported in part by the National Natural Science Foundation of China (NSFC) under Grant 41774132 and Grant 42074161, in part by the Hunan Provincial Innovation Foundation for Postgraduate under Grant CX20190216, and in part by the Graduate Independent Exploration and Innovation Project of Central South University under Grant 2019zzts160.

**ABSTRACT** The ground penetrating radar (GPR) data in the complex detection environment is non-stationary, non-Gaussian, and non-uniform, so the traditional noise attenuation methods are difficult to meet the requirements of denoising. Therefore, we introduced the K-singular value decomposition (K-SVD) dictionary learning into the denoising of GPR signals. It uses the orthogonal matching pursuit (OMP) algorithm to sparse decompose different radar data and trains the overcomplete dictionary with sample characteristics. K-SVD makes full use of the prior information and can extract features according to the sample data adaptively, which means it has strong sparse representation competence. Because radar signals can be sparsely represented in the dictionary, whereas the random noise does not have a sparse representation, the K-SVD dictionary can be used to distinguish effective signals from noise in the GPR data. We used the discrete cosine transform (DCT) and K-SVD dictionaries to process the Gaussian noise and stochastic clutter in the GPR profile. The results show that both K-SVD and DCT can effectively suppress the Gaussian noise. But for the clutter generated by the random medium, the DCT dictionary also causes damage to the effective signals while removing the noise; whereas the K-SVD dictionary learning algorithm uses the DCT dictionary as the initial dictionary and carries out adaptive learning on the noisy data, considering the information in the block and the global observation to complete the denoising, with good denoising effect and high fidelity. We finally verified the effectiveness and practicability of the K-SVD method for measured data.

**INDEX TERMS** Stochastic clutter suppression, dictionary learning, ground penetrating radar, K-singular value decomposition, noise attenuation.

## I. INTRODUCTION

Ground penetrating radar (GPR) is an important shallow geophysical exploration method, which has the advantages of high resolution, high efficiency, intuitive results, and non-destructive detection [1]. It is widely used in many fields such as sewage investigation, tunnel detection, engineering exploration, pipeline measurement, etc. [2]–[4]. Affected by complex geological conditions and the acquisition environment, GPR data is often accompanied by random noise and clutter interference, which greatly reduces the quality of radar data, even leads to signal distortion, and brings difficulties to

subsequent data processing and interpretation [5], [6]. Therefore, it is particularly important to study denoising methods to improve the signal-to-noise ratio (SNR) of GPR data.

At present, different scholars have proposed many methods to suppress the noise and improve the SNR of GPR. The famous soft-threshold using dyadic wavelets was proposed to optimally denoise and smooth signals in [7]. The wavelet transforms with different threshold functions were applied to GPR data, which effectively suppressed the noise and improved the SNR [8]. This algorithm is simple to implement, but it is difficult to select appropriate thresholds when the SNR is low. Fourier transform and wavelet transform, which are widely used in images, are also used in GPR noise attenuation and direct wave eliminating [9], [10]. However, it takes

The associate editor coordinating the review of this manuscript and approving it for publication was Francesco Benedetto .

a large amount of memory, so the computational efficiency is low [11]. F-K domain filtering is widely used in ringing noise and random noise removing of GPR profile [12], [13]. Curvelet transform is also used in noise suppression of GPR data due to its high flexibility and fast computational speed [14]–[17]. Empirical mode decomposition (EMD) was applied into many fields in processing geophysics signals [18]–[20], but it has the problem of mode mixing. In order to overcome this problem, ensemble EMD (EEMD) was proposed [21], [22]. However, EEMD cannot process raw data with low SNR [23]. Singular value decomposition (SVD) is a convenient method to decompose a matrix, which can decompose GPR data into different subspaces, and select components containing effective signals to reconstruct GPR signals [5], [24]. The authors in [25] proposed an SVD method based on the Hankel matrix in the local frequency domain for GPR, and handled different numerical models and field GPR data to eliminate the horizontal false signals effectively. On this basis, [26] provided a solution to optimize the size of the Hankel matrix, which can obtain the best noise removal performance for both white noise and correlated noise. However, the SVD method essentially cannot learn from the data and cannot be changed according to the characteristics of GPR signals. It can be seen that although these methods can suppress noise to a certain extent, they all have some shortcomings. In terms of removing clutter, principal component analysis (PCA) [27], independent component analysis (ICA) [28], morphological component analysis (MCA) [29], non-negative matrix factorization (NMF) [30], go decomposition (GoDec) [31], robust matrix factorization (RMF) [32], robust orthonormal subspace learning (ROSL) [33], robust PCA (RPCA) [34], [35], and tensor RPCA (TRPCA) [36], [37] are all good methods. They divide GPR data into two categories through different methods, one corresponding to the clutter and the other corresponding to the target signal, thus achieving the purpose of clutter removal. These methods are very effective for the largest clutter (direct wave), but are less effective for the removal of stochastic clutter generated by the underground random medium. For the removal of noise and this kind of stochastic clutter, traditional methods can no longer meet the requirements of interpretation accuracy. Therefore, this paper intends to adopt the dictionary denoising methods, train the dictionary with different radar data, and then apply it to the attenuation of GPR noise and stochastic clutter.

With the rapid development of GPR, the decoding of radar profiles has become more complicated. The method of self-denoising and stochastic clutter by learning data characteristics is more and more popular. The authors in [38] used artificial neural networks (ANN) to develop a regression model to estimate the signal-to-clutter ratio (SCR) for landmine detection using GPR. ANN has very strong independent learning competence, but it needs a lot of data for training and a diversity examination for training data [39]. However, in the actual detection of GPR, it is necessary to denoise and analyze the profile in real-time and make minor adjustments

to the next exploration plan. Therefore, ANN is not suitable for this fast denoising process. It has become a research hotspot nowadays that using the sparsity and separability of image data to remove the influence of noise [40]. The useful information in the image generally has sparseness, while the noise does not have this characteristic, so the noise can be removed from the image. This method is simple and fast, which is more in line with the requirements of rapid and accurate denoising.

Constructing an appropriate dictionary has become an important part for sparse representation [41]. The methods of constructing sparse dictionaries can be divided into two categories. One is to construct fixed structure dictionaries, the most typical of which is the discrete cosine transform (DCT) dictionary [42], [43]. The authors in [44] combined the DCT algorithm with the support vector machine (SVM) method to identify underground utilities from GPR images, and evaluated them under severe speckle noise effects, showing that the DCT method has better computational efficiency and accuracy in a noisy environment. The second category is to construct an adaptive redundant dictionary [45]. The authors developed Drop-Off MINI-batch Online Dictionary Learning (DOMINODL) for GPR, which exploits the fact that a lot of the training data may be correlated in [41]. This algorithm is fast, but requires more input parameters. The K-Singular value decomposition (K-SVD) algorithm in [46] is the most representative and most widely used adaptive learning dictionary algorithm. On this basis, an overcomplete dictionary with adaptive learning ability was constructed to sparsely decompose the target image, achieving the purpose of eliminating the image noise [47]. In [48], the authors proposed a new K-SVD method, called Graph K-SVD, to consider the manifold structure of the data. It makes full use of the intrinsic geometrical information and iterative methods to solve the optimization problem, which has good robustness to the error threshold. In [49], the authors proposed an implementation of distributed parallel optimization of the K-SVD algorithm on Spark, which not only has a good speed-up ratio, but also retains the image texture and other details. The overcomplete dictionary was applied to seismic denoising in [50] and compared with traditional transform basis function denoising methods. The authors in [51] proposed an adaptive sparse decomposition for GPR signal analysis and classification to extract salient features. Nowadays, it is still rare to apply the K-SVD algorithm for GPR noise removal or clutter suppression.

In this paper, sparse decomposition theory is applied to GPR denoising, and an ideal K-SVD dictionary is trained by given different radar data. By comparing the adaptive redundant K-SVD dictionary with the DCT dictionary for radar random noise and clutter suppression, it is shown that both dictionary algorithms can effectively distinguish useful wave information from random disturbance, and achieve noise attenuation of GPR data. Besides, the K-SVD dictionary algorithm can make full use of the prior information, and extract features based on the sample data adaptively.

It has better sparse representation competence, better effect in clutter interference suppression, and better data fidelity than the DCT dictionary.

## II. THEORETICAL FRAMEWORK

In the conventional denoising methods of GPR data, a set of fixed transform basis functions are generally adopted, which are not adjusted according to the characteristics of data, so the denoising effect is not ideal. In recent years, dictionary learning methods that can adaptively change the basis function according to data have been proposed. Because radar signals can have a sparse representation in the dictionary, whereas random noise does not. Thus, the dictionary learning method can realize the separation of noise and effective signals, and achieve the purpose of denoising.

To better understand the sparse representation and the K-SVD algorithm, we put the important symbols and their meanings in Table 1.

TABLE 1. Symbols and meanings.

Symbol	Meaning
$\mathbf{Y}$	the signal of size $M \times N$
$\mathbf{D}$	the overcomplete dictionary of size $M \times K$ ( $K > M$ )
$\mathbf{X}$	the sparse representation of size $K \times N$
$\mathbf{d}_k$	the dictionary atom, i.e., the $k$ th column of $\mathbf{D}$
$\mathbf{x}_k^t$	the corresponding sparse coefficients to $\mathbf{d}_k$ , the $k$ th row in $\mathbf{X}$
$\mathbf{E}_k$	the error matrix of size $M \times N$
$\Omega_k$	an index matrix pointing to the positions of nonzero elements
$\ \cdot\ _0$	$l_0$ norm, counting the nonzero entries of a vector
$\ \cdot\ _1$	$l_1$ norm, the sum of the absolute values of the vector
$\ \cdot\ _F$	Frobenius norm, defined as $\ \mathbf{A}\ _F = \sqrt{\sum_{ij} A_{ij}^2}$

### A. THE PRINCIPLE FOR SPARSE REPRESENTATION

The image with noise can be modeled as  $\mathbf{Y} = \mathbf{G} + \mathbf{C}$ , where  $\mathbf{Y}$  is the noisy image,  $\mathbf{C}$  is the noise,  $\mathbf{G}$  is the original image. The denoising process includes two key steps, the sparse decomposition of signals and the construction of overcomplete dictionaries.

Given a matrix  $\mathbf{D} = [\mathbf{d}_1, \mathbf{d}_2, \dots, \mathbf{d}_K] \in \mathfrak{R}^{M \times K} = \{\mathbf{d}_k\}_{k=1}^K$  of size  $M \times K$  (where  $K \gg M$ ), each column  $\mathbf{d}_k$  can be regarded as a dictionary atom. For any given vector  $\mathbf{Y} = \{\mathbf{y}_m\}_{m=1}^M$ , the problem to be studied for sparse representation is to find a sparse coefficient vector  $\mathbf{X}$  of size  $K \times 1$ , so that the signals  $\mathbf{Y}$  can be regarded as a linear combination of a series of atoms, i.e.,  $\mathbf{Y} = \mathbf{D}\mathbf{X}$ . Since  $K \gg M$ ,  $\mathbf{D}$  is a full-rank matrix, representing an infinite number of solutions are available for the representational problem. The solution with the fewest number of nonzero elements is the most appropriate. It can be expressed as [52]

$$\min \|\mathbf{X}\|_0 \quad s.t. \quad \mathbf{Y} = \mathbf{D}\mathbf{X} \quad (1)$$

For the optimization of the solution, since the  $l_0$  norm has the convexification problem, the usual approach is to transform the  $l_0$  norm constraint problem into the  $l_1$  norm to

solve, namely

$$\min \|\mathbf{X}\|_1 \quad s.t. \quad \mathbf{Y} = \mathbf{D}\mathbf{X} \quad (2)$$

When the sparsity of the solution is very high, the two solutions are equivalent. In order to represent the signal sparsely, the sparse model needs to be estimated first.

### B. SPARSE REPRESENTATION

The process of sparse decomposition is mainly to obtain the optimal sparse representation form of the signal under dictionary constraints, which can also be regarded as the realization of the sparse representation of the signal. In this paper, we used the orthogonal matching pursuit (OMP) algorithm to realize the sparse decomposition of signals [53]. The OMP algorithm is an improvement of the MP algorithm, which uses Gram-Schmidt orthogonalization to normalize the projection direction. Given the dictionary  $\mathbf{D} = \{\mathbf{d}_k\}_{k=1}^K$  and  $\|\mathbf{d}_k\|_2^2 = 1$ , the decomposition process of signal  $\mathbf{Y}$  using the OMP algorithm is as follows [54]. Set the initial value  $\mathbf{r}_0 = \mathbf{Y}$ , an empty dictionary set  $\mathbf{S}_0$ , and then find the subscript  $\lambda_1$  corresponding to the largest inner product of the residual  $\mathbf{r}_0$  and a column  $\mathbf{d}_k$  in the dictionary  $\mathbf{D}$ , i.e.,

$$\lambda_1 = \arg \max_{k=1, \dots, K} |\langle \mathbf{r}_0, \mathbf{d}_k \rangle| \quad (3)$$

Add  $\mathbf{d}_{\lambda_1}$  to the dictionary  $\mathbf{S}_0$ , rename it as  $\mathbf{S}_1$ . Then, the least square method is used to calculate the sparse representation  $\mathbf{X}_1$

$$\mathbf{X}_1 = \arg \min \|\mathbf{Y} - \mathbf{S}_1\mathbf{X}\| \quad (4)$$

Calculate the new residual  $\mathbf{r}_1$ ,

$$\mathbf{r}_1 = \mathbf{Y} - \mathbf{S}_1\mathbf{X}_1 \quad (5)$$

In the remaining dictionary  $\mathbf{D}$ , find  $\mathbf{d}_{\lambda_2}$  which has the largest inner product with the residual  $\mathbf{r}_1$ . Put  $\mathbf{d}_{\lambda_2}$  into the dictionary  $\mathbf{S}_1$ , update it to  $\mathbf{S}_2$ , and also use the least square method to calculate  $\mathbf{X}_2$

$$\mathbf{X}_2 = \arg \min \|\mathbf{Y} - \mathbf{S}_2\mathbf{X}\| \quad (6)$$

Using  $\mathbf{X}_2$ , we calculate the new residual  $\mathbf{r}_2$

$$\mathbf{r}_2 = \mathbf{Y} - \mathbf{S}_2\mathbf{X}_2 \quad (7)$$

After  $K$  iterations of the above process, we can get the final sparse representation  $\mathbf{X}_K$ .

### C. OVERCOMPLETE DICTIONARY CONSTRUCTION

#### 1) DCT OVERCOMPLETE DICTIONARY

The DCT dictionary has a good ability to decompose periodic signals. For the two-dimensional signal  $\mathbf{Y}$  of size  $M \times N$ , its two-dimensional DCT transform can be written as

$$F(u, v) = c(u)c(v) \sum_{i=0}^{M-1} \sum_{j=0}^{N-1} Y(i, j) \times \cos \left[ \frac{(2i+1)\pi}{2M}u \right] \cos \left[ \frac{(2j+1)\pi}{2N}v \right] \quad (8)$$

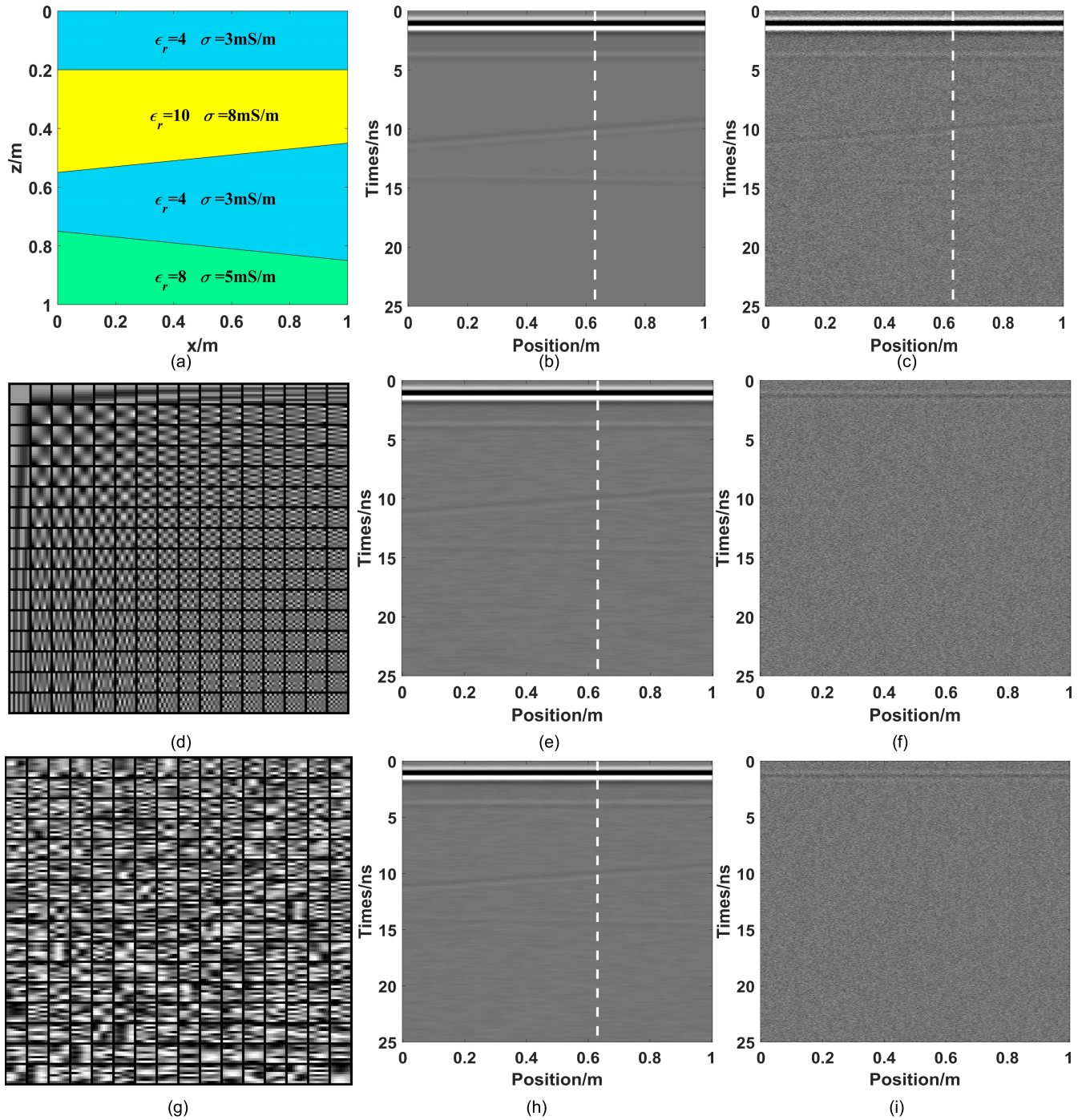


**FIGURE 1.** Schematic diagram of the layered model and denoising results of different methods. (a) is the layered model, (b) is the original forward profile, (c) is the radar profile with the Gaussian noise, (d) is the DCT dictionary, (e) is the denoising profile with the DCT dictionary, (f) is the residual between (c) and (e), (g) is the K-SVD dictionary, (h) is the denoising profile with the K-SVD dictionary, (i) is the residual between (c) and (h).

where,  $u = 0, 1, 2, \dots, M - 1$ ;  $v = 0, 1, 2, \dots, N - 1$ ;  $F(u, v)$  is the DCT coefficient;  $c(u)$  and  $c(v)$  are the compensation coefficients, and are defined as

$$c(u) = \begin{cases} \sqrt{\frac{1}{M}} & u = 0 \\ \sqrt{\frac{2}{M}} & u \neq 0 \end{cases},$$

$$c(v) = \begin{cases} \sqrt{\frac{1}{N}} & v = 0 \\ \sqrt{\frac{2}{N}} & v \neq 0 \end{cases} \quad (9)$$

For the complete dictionary obtained after the DCT transformation, the fractional frequency method is adopted to expand it into an overcomplete dictionary. The specific

method is to get a new overcomplete dictionary by making more fine convenience and sampling on the frequency.

## 2) K-SVD DICTIONARY LEARNING

The K-SVD algorithm is mainly used to find an overcomplete dictionary  $\mathbf{D} \in \mathfrak{R}^{M \times K}$  and a sparse coefficient matrix  $\mathbf{X} \in \mathfrak{R}^{K \times N}$ . Assuming that  $\mathbf{Y} \in \mathfrak{R}^{M \times N}$  is a given set of sample signals, the objective function can be expressed as [55]

$$\min \|\mathbf{Y} - \mathbf{D}\mathbf{X}\|_F^2 \quad s.t. \quad \forall i, \quad \|\mathbf{x}_i\|_0 \leq T_0 \quad (10)$$

$T_0$  is the number of nonzero elements required in advance. The K-SVD dictionary in this paper takes the DCT dictionary as the initial dictionary, and uses the OMP algorithm to get the sparse representation  $\mathbf{X}$  corresponding to the DCT dictionary at this time. Then the K-SVD algorithm is used to update the overcomplete dictionary  $\mathbf{D}$  and sparse representation  $\mathbf{X}$ .

When carrying out the task of dictionary atomic update, any atom  $\mathbf{d}_k$  in the dictionary is updated in order. At the same time, the corresponding sparse coefficient vector, the  $k$ th row in  $\mathbf{X}$ ,  $\mathbf{x}_T^k$  are calculated (this is not the vector  $\mathbf{x}_k$  which is the  $k$ th column in  $\mathbf{X}$ ). The objective function can be expressed as [46]

$$\begin{aligned} \|\mathbf{Y} - \mathbf{D}\mathbf{X}\|_F^2 &= \left\| \mathbf{Y} - \sum_{j=1}^K \mathbf{d}_j \mathbf{x}_T^j \right\|_F^2 \\ &= \left\| \left( \mathbf{Y} - \sum_{j \neq k} \mathbf{d}_j \mathbf{x}_T^j \right) - \mathbf{d}_k \mathbf{x}_T^k \right\|_F^2 \\ &= \left\| \mathbf{E}_k - \mathbf{d}_k \mathbf{x}_T^k \right\|_F^2 \end{aligned} \quad (11)$$

The main task of a dictionary update is to perform the SVD operation on the error matrix  $\mathbf{E}_k$  generated by the atom in the  $k$ th column of the dictionary, i.e.,

$$\mathbf{E}_k = \mathbf{Y} - \sum_{j \neq k} \mathbf{d}_j \mathbf{x}_T^j \quad (12)$$

The matrix  $\mathbf{D}\mathbf{X}$  will be transformed into the sum of  $K$  matrices of rank-1, and the SVD will find the closest rank-1 matrix that approximates  $\mathbf{E}_k$ . However, such a step will be a mistake, because the new vector  $\mathbf{x}_T^k$  is very likely to be filled, causing its nonzero elements to be in a different position. Define  $\omega_k$  as the group of indices pointing to the positions those where  $\mathbf{x}_T^k(i)$  is nonzero. so there is

$$\omega_k = \left\{ i \mid 1 \leq i \leq K, \mathbf{x}_T^k(i) \neq 0 \right\} \quad (13)$$

Define  $\Omega_k$  as a matrix of size  $N \times |\omega_k|$ , with ones on the  $(\omega_k(i), i)$  th entries and 0 elsewhere. Multiply Eq. (11) by the limiting factor  $\Omega_k$ , then we can get

$$\left\| \mathbf{E}_k \Omega_k - \mathbf{d}_k \mathbf{x}_T^k \Omega_k \right\|_F^2 = \left\| \mathbf{E}_k^R - \mathbf{d}_k \mathbf{x}_R^k \right\|_F^2 \quad (14)$$

Perform SVD decomposition on  $\mathbf{E}_k^R$  to obtain  $\mathbf{E}_k^R = \mathbf{U}\mathbf{\Delta}\mathbf{V}^T$ . Replace  $\mathbf{d}_k$  with the first column of  $\mathbf{U}$ , and use

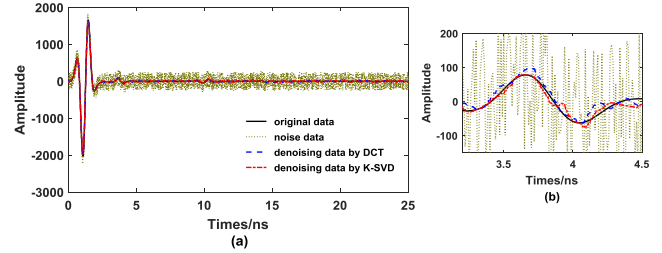


**FIGURE 2.** A-scan comparison of denoising results. The black solid line represents the original A-scan, the other dotted line represents the noise data, the blue dashed line represents the denoising result of the DCT dictionary, and the red chain-dotted line represents the denoising result of the K-SVD dictionary. (a) is the overall picture; (b) is the partial enlargement of (a).

the product  $\mathbf{x}_k^R$  of the first column of  $\mathbf{V}$  and  $\mathbf{\Delta}(1, 1)$  as the sparse coefficient matrix. Thus, we can obtain the sparse representation of signals in the K-SVD dictionary.

## III. THE DENOISING OF SYNTHETIC GPR DATA

To analyze the denoising effect of the dictionary learning algorithms, two typical types of noise data in the GPR signal are selected: (a) signal interference caused by the instrument itself or system noise; (b) stochastic clutter generated by the underground random medium. Two different models are selected to conduct experiments on these two types of noise. The synthetic data are generated by using the finite-difference time-domain (FDTD) method to simulate.

All tests are performed in a 64-bit Ubuntu 20.04.1 LTS environment. The CPU environment is Inter (R) Core (TM) i7-6700K CPU @ 4.00GHz  $\times$  8, and the codes are run in anaconda python 3.8.

### A. SYSTEM NOISE DENOISING ANALYSIS

First, we considered the signal interference caused by the instrument itself or system noise, which is similar to Gaussian white noise. We established a layered model as shown in Fig. 1(a). The simulation area is 1 m  $\times$  1 m, the relative permittivity of the model is 4, 10, 4, and 8 from top to bottom, and the conductivity is 3 mS/m, 8 mS/m, 3 mS/m, and 5 mS/m in turn. The discrete mesh of the model is 200  $\times$  200, the mesh interval is 0.005 m, and 10-layer CPML was used as the absorption boundary. The Ricker wavelet with the main frequency of 900 MHz was placed on the ground as the source pulse. The simulation window is 25 ns and the sampling interval is 0.01 ns. The FDTD algorithm was used to forward the model, and a total of 178 channels of data were received, with the track interval of 0.005 m and the transceiver interval of 0.01 m. Fig. 1(b) is the original forward profile. We added the Gaussian noise to the forward profile, as shown in Fig. 1(c). The comparison between the two shows that the profile data with the Gaussian noise has a great influence on the original data, and the reflected waves are almost annihilated.

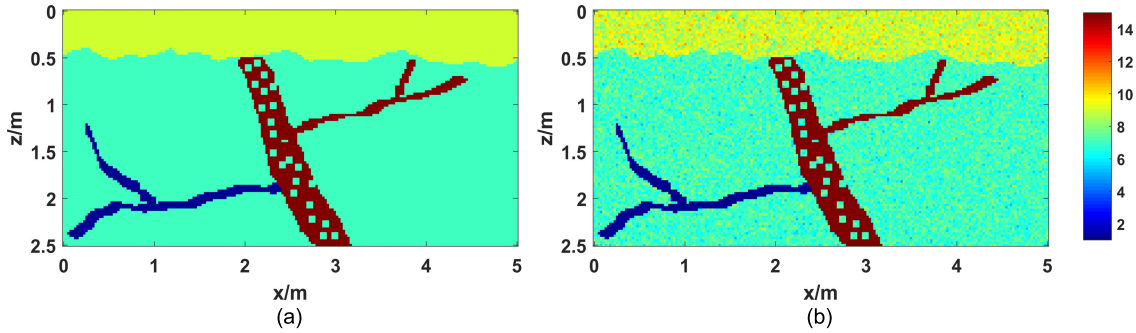


**FIGURE 3.** The diagram of the water-bearing lining model. (a) The background is a homogeneous medium; (b) The background is a random medium.

To describe the noise level more clearly, the SNR calculation formula shown in Eq. (15) is introduced [56]

$$SNR = 10 \log_{10} \left[ \frac{\sum_{x=1}^{N_x} \sum_{y=1}^{N_y} (f(x, y))^2}{\sum_{x=1}^{N_x} \sum_{y=1}^{N_y} (f(x, y) - \hat{f}(x, y))^2} \right] \quad (15)$$

where,  $N_x$  and  $N_y$  are the size of the image, i.e., the size of the image is  $N_x \times N_y$ ;  $f(x, y)$  is the original image,  $\hat{f}(x, y)$  is the noisy image. The smaller the difference between the original image and the noisy image, the lower the noise level and the higher the SNR. Therefore, a high SNR indicates a better denoising effect, and a low SNR indicates a poor denoising effect. The SNR of the noisy image in Fig. 1(c) is 4.8225, indicating high noise.

The DCT overcomplete dictionary does not need to learn from data, only needs to use the fractional frequency method to expand, as shown in Fig. 1(d). All the K-SVD dictionaries in this paper are first selected the DCT dictionary as an initial dictionary, and then given experimental data samples, training and learning according to the sparse constraint conditions, so as to update the dictionary with the noisy data atomically. It can extract features from sample data adaptively, realize the maximum sparsity of the original signal, and finally obtain a redundant K-SVD overcomplete dictionary. Therefore, the K-SVD dictionary can be adaptive to update the dictionary according to the characteristics of noise data, and has strong adaptability. The K-SVD dictionary trained in this example is shown in Fig. 1(g).

Fig. 1(e) is the denoising profile of the DCT dictionary, and its residual is shown in Fig. 1(f). The running time of the DCT denoising algorithm is 4.85 s. By comparing Fig. 1(c) and Fig. 1(e), the denoising process using the DCT overcomplete dictionary can effectively suppress the Gaussian noise, and the reflected wave information can be clearer. The SNR calculated by Eq. (15) is 23.3727, which is greatly improved compared with the noisy data. The residual results shown in Fig. 1(f) show that the DCT overcomplete dictionary can remove the Gaussian noise well, and the reflected wave does not appear in the residual profile, indicating that the algorithm

has less damage to the reflected waves. Fig. 1(g) shows the overcomplete dictionary of the K-SVD algorithm, which is learned from the noisy data (Fig. 1(c)). The denoising profile of K-SVD is shown in Fig. 1(h), and the residual is shown in Fig. 1(i). The running time of the K-SVD denoising algorithm is 26.85 s. The time is slightly longer than DCT, because the K-SVD algorithm needs to learn from the data to update the dictionary. By comparing Fig. 1(c) and Fig. 1(h), it can be seen that the K-SVD dictionary has a good effect on the data denoising, and the reflected waves can be distinguished in the profile. The SNR calculated by Eq. (15) is 23.4133, which is approximately consistent with the DCT method. By observing the residual results shown in Fig. 1(i), it can also be found that the K-SVD overcomplete dictionary has a good denoising effect, and the residuals are all random and irregular Gaussian noise.

In order to observe the denoising results more intuitively, the denoising results of the 112th A-scan data (white dashed line) are selected for analysis, and the results are shown in Fig. 2(a). The black solid line represents the original A-scan data, and the other dotted line represents the noise data. The denoised reflection waveform of the DCT dictionary indicated by the blue dashed line corresponds well to the original data and does not interfere with the effective information. The overall denoising effect of the K-SVD dictionary represented by the red chain-dotted line is not much different from that of the DCT overcomplete dictionary. The amplitude of A-scan data after denoising by the two methods are approximately the same as the original A-scan, which indicates that they both can effectively suppress the Gaussian noise and realize the denoising of noisy radar data. From Fig 2(b), K-SVD is closer to the original data in amplitude than DCT, and both of them appear oscillation phenomenon. Therefore, any kind of denoising method can be used to remove the Gaussian noise.

### B. RANDOM MEDIUM CLUTTER ANALYSIS

In the exploration with GPR, clutter will be generated due to the underground random medium. In order to explain the effect of the dictionary learning algorithm on removing clutter in detail, a water-bearing lining model with

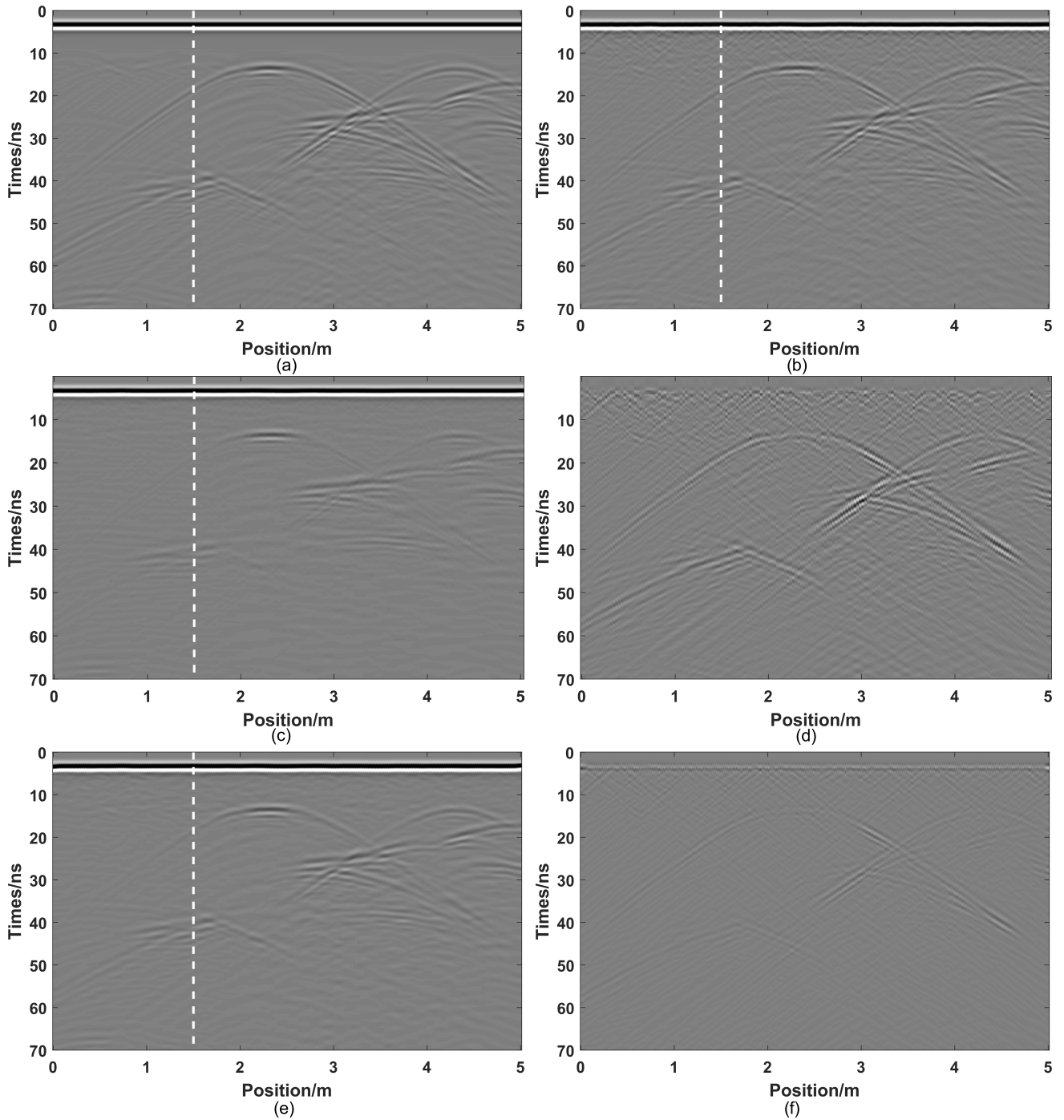


**FIGURE 4.** Forward GPR profiles and denoising results by different methods. (a) is the forward profile of the water-bearing lining model with the uniform background medium, (b) is the forward profile of the model with the random background medium, (c) is the denoising profile with the DCT dictionary, (d) is the residual between (b) and (c), (e) is the denoising profile with the K-SVD dictionary, (f) is the residual between (b) and (e).

a homogeneous background as shown in Fig. 3(a) was established, and the random medium was constructed by an exponential elliptic autocorrelation function as shown in Fig. 3(b). Its function expression is [57], [58]

$$\phi(x, z) = \exp \left[ -\sqrt{(x^2/a^2 + z^2/b^2)} \right] \quad (16)$$

where,  $a$  and  $b$  represent the autocorrelation length of the medium in the  $x$  and  $z$  directions respectively. In Fig. 3(b),  $a = b = 0.025$  m, the variance is 0.2, and the mean value is the background medium value. The other model parameters are consistent with those in Fig. 3(a). The simulation area is  $5 \text{ m} \times 2.5 \text{ m}$ . The discrete mesh of the model is  $200 \times 100$ , the mesh interval is 0.025 m, and 10-layer CPML was used

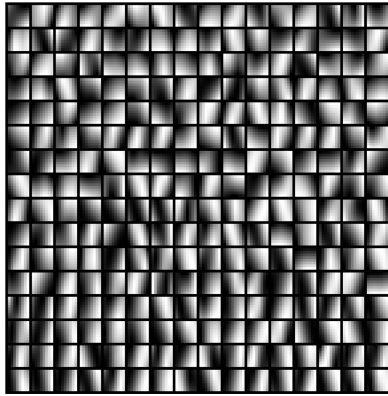


FIGURE 5. Overcomplete dictionary based on the K-SVD learning.

as the absorption boundary. The Ricker wavelet with the main frequency of 400 MHz was placed on the ground as the source pulse. The simulation window is 70 ns and the sampling interval is 0.01 ns. The FDTD algorithm was used to forward the model, and a total of 176 channels of data were received, with the track interval of 0.025 m and the transceiver interval of 0.1 m. Fig. 4 (a) and Fig. 4(b) show the forward profile of water-bearing lining model with a uniform background medium and a random background medium, respectively.

The overcomplete DCT dictionary shown in Fig. 1(d) was also used for denoising in this example. The denoising profile is shown in Fig. 4(c) and the residual is shown in Fig. 4(d). The running time of the DCT denoising algorithm is 5.92 s. By comparing Fig. 4(c) and Fig. 4(b), it can be found that the DCT dictionary can suppress random interference and reduce clutter to a certain extent. However, by observing Fig. 4(d), it can be seen that the profile processed by the DCT overcomplete dictionary has a serious loss of effective information while removing the clutter. The K-SVD dictionary also selects the DCT dictionary as the initial dictionary, and then performs the update of the dictionary through the random medium radar forward data (Fig. 4(b)), and finally obtains an overcomplete dictionary as shown in Fig. 5. The denoising profile of the K-SVD dictionary is shown in Fig. 4(e), and the residual of it is shown in Fig. 4(f). The running time of the K-SVD denoising algorithm is 31.85 s. By comparing Fig. 4(b) with Fig. 4(e), the K-SVD dictionary can suppress random noise to a large extent, and the reflected wave information is clearer. Besides, by analyzing the residual results in Fig. 4(f), compared with the denoising of the DCT dictionary, the K-SVD dictionary is less destructive to the effective wave information relatively, and the denoising effect is significantly improved.

In order to observe the denoising results more intuitively, we selected the A-scan at the white dashed line in Fig. 4 for analysis, and the results are shown in Fig. 6(a). It can be seen from the figure that the K-SVD dictionary and the DCT dictionary denoising algorithms are approximately consistent with the original data. From the partial enlargements Fig. 6(b), we can see that the noise is oscillating compared

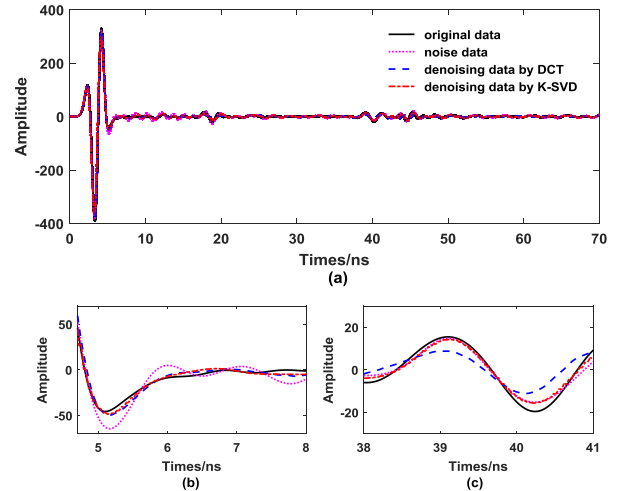


FIGURE 6. A-scan comparison of denoising results. The black solid line represents the original A-scan, the pink dotted line represents the noise data, the blue dashed line represents the denoising result of the DCT dictionary, and the red chain-dotted line represents the denoising result of the K-SVD dictionary. (a) is the overall picture; (b) and (c) are the partial enlargements of (a).

with the original data, and both the A-scan of K-SVD and DCT show a good denoising effect. However, it can be seen from Fig. 6(c) that the K-SVD dictionary method algorithm is closer to the original data in amplitude than DCT, indicating that it retains effective information better and does less damage to the original profile.

#### IV. THE DENOISING OF MEASURED GPR DATA

The measured data is located in the access tunnel of the Heimifeng Pumped-storage Power Station in Hunan Province, China. The total length is 996 m, and the excavated section is about 7.8 m high and 8.4 m wide. During the operation of the traffic tunnel, there have been many times when the top arch has fallen off. Effective measures must be taken to identify the weak parts of the surrounding rock to strengthen the support and ensure the safety of the traffic tunnel. In this paper, we select the unlined pile number  $J_0 + 330 \text{ m} - J_0 + 350 \text{ m}$  shown in Fig. 7(a) as the denoising experiment data. The data is noisy data interfered by telecom base stations. GSSI-3000 GPR was used for data acquisition. The main frequency of the antenna is 900 MHz, the length of the survey line is 200 m, the interval of measuring points is 0.4 m, and the recording time is 40 ns.

Fig. 8 is the K-SVD overcomplete dictionary obtained after learning the original profile in Fig. 7(a). The denoising result is shown in Fig. 7(b) and Fig. 7(c) is the residual. The running time of the K-SVD denoising algorithm for measured data is 497.70 s. It can be seen from Fig. 7(b) that the GPR profile denoised by the K-SVD dictionary learning algorithm not only removes the Gaussian noise well, but also loses less effective information. Most of the noise is suppressed, the anomaly is more obvious, and the SNR is significantly improved. The location enclosed by the red circle is

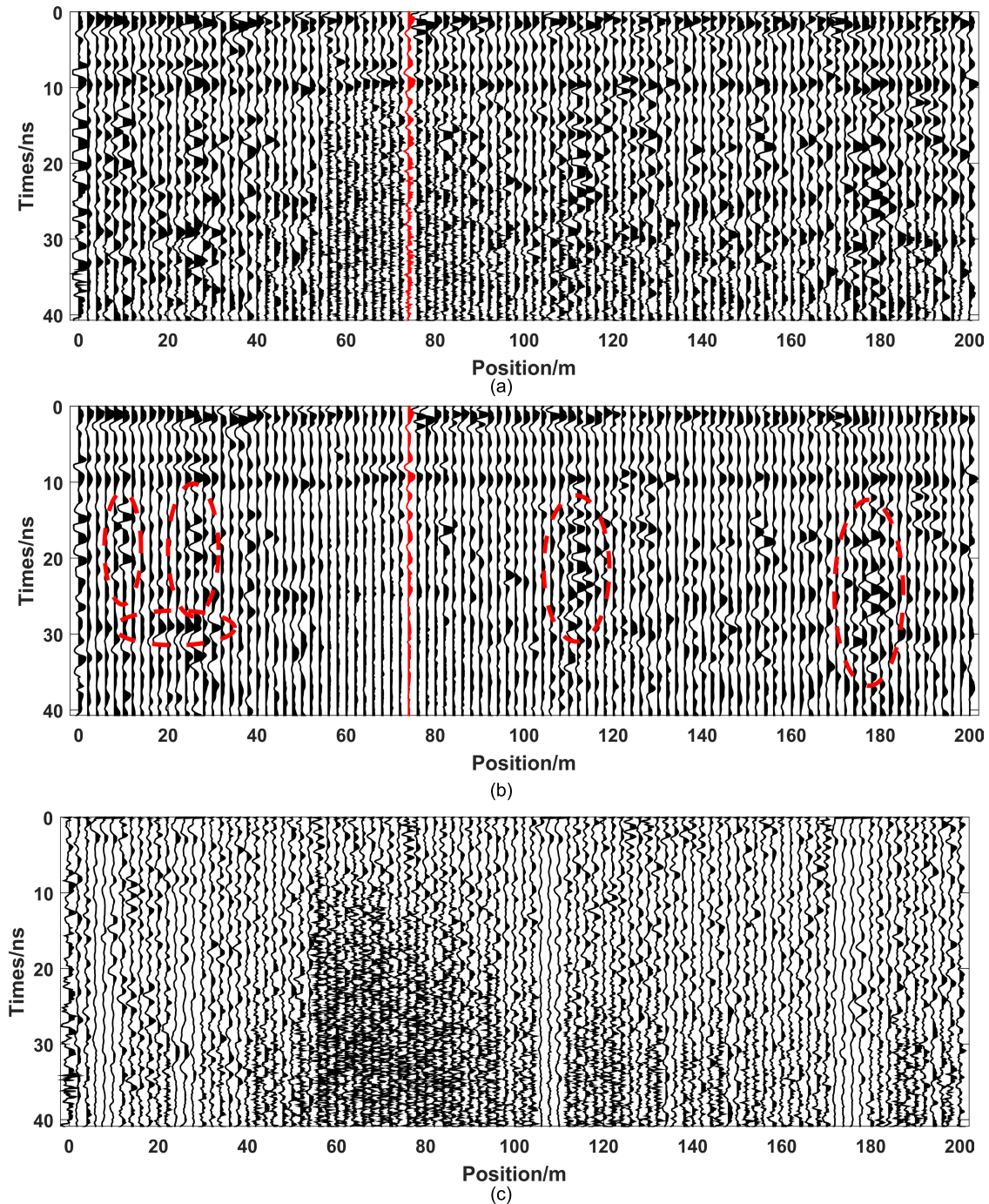


**FIGURE 7.** The measured data profile and denoising results. (a) is the original profile of the measured data, (b) is the denoising profile with the K-SVD dictionary, (c) is the residual between (a) and (b).

preliminarily estimated to be the partial fracture and fissure of rocks in the tunnel. In the analysis of Fig. 7(c), it is also found that the K-SVD dictionary learning algorithm eliminates the noise and does not weaken the effective information too much, most of which is random noise.

In order to further illustrate the denoising effect of the K-SVD algorithm on the measured data, the A-scan of the

data denoising results at the red track were compared with the original data. By analyzing the A-scan radar data shown in Fig. 9, it can be found that before 25 ns, the denoising profile approximately coincides with the original profile, and the curve trend is the same, but after 25 ns, the original profile is full of noise, whereas the amplitude of the K-SVD denoising A-scan data decreases, indicating that the K-SVD

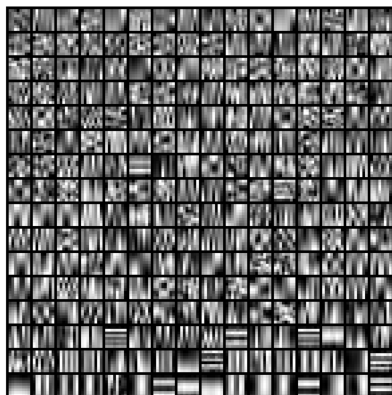


FIGURE 8. K-SVD learning dictionary for measured data.

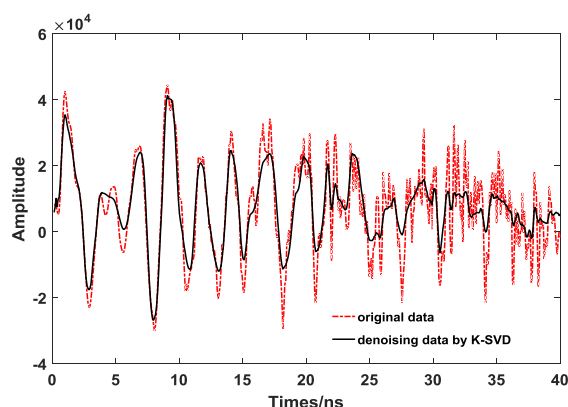


FIGURE 9. The denoising result of measured data. The red dashed line is the measured data, and the black solid line is the denoising result of K-SVD.

dictionary learning denoising algorithm can better identify effective information and noise data, and most of the noise that oscillates up and down can be well suppressed.

## V. CONCLUSION

In the conventional GPR data denoising processing, a fixed transform basis is used to process the radar data, and the denoising effect is not ideal. The effective information of radar data can be represented in the dictionary sparsely, whereas the random noise is tiled in the entire sparse domain and cannot be sparsely represented in the dictionary. According to this characteristic, we proposed to apply the K-SVD dictionary learning algorithm to radar data processing, effectively separating the effective information and noise.

The K-SVD dictionary learning denoising method, with the DCT dictionary as the initial dictionary, can be adaptively updated according to the characteristics of the radar data itself. According to the sparse constraint conditions, it continuously updates the dictionary and sparse coefficients alternately through the SVD of the difference between the reconstructed signal and the original signal. Therefore, an overcomplete dictionary that meets the characteristics of the data can be trained to realize the sparse representation of

the radar data, so as to maximize the separation of noise and effective signals and achieve the purpose of denoising.

For the Gaussian noise and clutter interference added to the synthetic radar data, two learning denoising algorithms, the DCT dictionary and the K-SVD dictionary, were respectively used for denoising comparison experiments, indicating that both algorithms can effectively remove the Gaussian noise. For the clutter interference generated by random media, compared with the DCT dictionary, the K-SVD dictionary learning denoising algorithm can significantly reduce the damage to the effective signal while removing the clutter. It is a very potential adaptive GPR interference removal algorithm, and the denoising results of the measured radar data also verify this conclusion.

In our future work, we intend to further study the K-SVD algorithm, improve its denoising effect, and compare it with other algorithms to promote the development of GPR data processing and interpretation.

## ACKNOWLEDGMENT

The authors would like to thank the editors and anonymous reviewers for their critical reviews and valuable comments.

## REFERENCES

- [1] M. Yang, H. Fang, F. Wang, H. Jia, J. Lei, and D. Zhang, "The three dimension first-order symplectic partitioned Runge-Kutta scheme simulation for GPR wave propagation in pavement structure," *IEEE Access*, vol. 7, pp. 151705–151712, Oct. 2019.
- [2] N. Diamanti, A. P. Annan, and J. D. Redman, "Concrete bridge deck deterioration assessment using ground penetrating radar (GPR)," *J. Environ. Eng. Geophys.*, vol. 22, no. 2, pp. 121–132, Jun. 2017.
- [3] N. Bonomo, M. de la Vega, P. Martinelli, and A. Osella, "Pipe-flange detection with GPR," *J. Geophys. Eng.*, vol. 8, no. 1, pp. 35–45, Mar. 2011.
- [4] J. Xiao and L. Liu, "Permafrost subgrade condition assessment using extrapolation by deterministic deconvolution on multifrequency GPR data acquired along the Qinghai-Tibet railway," *IEEE J. Sel. Topics Appl. Earth Observ. Remote Sens.*, vol. 9, no. 1, pp. 83–90, Jan. 2016.
- [5] C. Liu, C. Song, and Q. Lu, "Random noise de-noising and direct wave eliminating based on SVD method for ground penetrating radar signals," *J. Appl. Geophys.*, vol. 144, pp. 125–133, Sep. 2017.
- [6] T. Ling, L. Zhang, H. Liu, D. Gu, B. Yu, and S. Zhang, "OMWS method for weak signal processing of GPR and its application in the identification of concrete microcracks," *J. Environ. Eng. Geophys.*, vol. 24, no. 2, pp. 317–325, Jun. 2019.
- [7] D. L. Donoho, "De-noising by soft-thresholding," *IEEE Trans. Inf. Theory*, vol. 41, no. 3, pp. 613–627, May 1995.
- [8] B. Oskooi, M. Julayusefi, and A. Goudarzi, "GPR noise reduction based on wavelet thresholdings," *Arabian J. Geosci.*, vol. 8, no. 5, pp. 2937–2951, Mar. 2014.
- [9] J. Baili, S. Lahouar, M. Hergli, I. L. Al-Qadi, and K. Besbes, "GPR signal de-noising by discrete wavelet transform," *NDT & E Int.*, vol. 42, no. 8, pp. 696–703, Dec. 2009.
- [10] M. Javadi and H. Ghasemzadeh, "Wavelet analysis for ground penetrating radar applications: A case study," *J. Geophys. Eng.*, vol. 14, no. 5, pp. 1189–1202, Oct. 2017.
- [11] R. Neelamani, A. I. Baumstein, D. G. Gillard, M. T. Hadidi, and W. L. Soroka, "Coherent and random noise attenuation using the curvelet transform," *Lead. Edge*, vol. 27, no. 2, pp. 240–248, Feb. 2008.
- [12] J.-H. Kim, S.-J. Cho, and M.-J. Yi, "Removal of ringing noise in GPR data by signal processing," *Geosci. J.*, vol. 11, no. 1, pp. 75–81, Mar. 2007.
- [13] X. Zhang, X. Feng, Z. Zhang, Z. Kang, Y. Chai, Q. You, and L. Ding, "Dip filter and random noise suppression for GPR B-scan data based on a hybrid method in f-x domain," *Remote Sens.*, vol. 11, no. 18, p. 2180, Sep. 2019.

- [14] G. Terrasse, J.-M. Nicolas, E. Trouvé, and É. Drouet, "Application of the curvelet transform for clutter and noise removal in GPR data," *IEEE J. Sel. Topics Appl. Earth Observ. Remote Sens.*, vol. 10, no. 10, pp. 4280–4294, Oct. 2017.
- [15] T. He and H. Shang, "Direct-wave denoising of low-frequency ground-penetrating radar in open pits based on empirical curvelet transform," *Near Surf. Geophys.*, vol. 18, no. 3, pp. 295–305, Jun. 2020.
- [16] Z.-Y. Zhang, X.-D. Zhang, H.-Y. Yu, and X.-H. Pan, "Noise suppression based on a fast discrete curvelet transform," *J. Geophys. Eng.*, vol. 7, no. 1, pp. 105–112, Mar. 2010.
- [17] Q. Bao, Q. Li, and W. Chen, "GPR data noise attenuation on the curvelet transform," *Appl. Geophys.*, vol. 11, pp. 301–310, Nov. 2014.
- [18] Q. Lu, C. Liu, and X. Feng, "Signal enhancement of GPR data based on empirical mode decomposition," in *Proc. 15th Int. Conf. Ground Penetrating Radar (GPR)*, Jun. 2014, pp. 683–686.
- [19] B. M. Battista, A. D. Addison, and C. C. Knapp, "Empirical mode decomposition operator for dewowing GPR data," *J. Environ. Eng. Geophys.*, vol. 14, no. 4, pp. 163–169, Dec. 2009.
- [20] R. Ostoori, A. Goudarzi, and B. Oskooi, "GPR random noise reduction using BPD and EMD," *J. Geophys. Eng.*, vol. 15, no. 2, pp. 347–353, Apr. 2018.
- [21] W. Xue, X. Dai, J. Zhu, Y. Luo, and Y. Yang, "A noise suppression method of ground penetrating radar based on EEMD and permutation entropy," *IEEE Geosci. Remote Sens. Lett.*, vol. 16, no. 10, pp. 1625–1629, Oct. 2019.
- [22] L. Gan, L. Zhou, and S. M. Liu, "A de-noising method for GPR signal based on EEMD," *Appl. Mech. Mater.*, vols. 687–691, pp. 3909–3913, Nov. 2014.
- [23] J. Li, C. Liu, Z. Zeng, and L. Chen, "GPR signal denoising and target extraction with the CEEMD method," *IEEE Geosci. Remote Sens. Lett.*, vol. 12, no. 8, pp. 1615–1619, Aug. 2015.
- [24] F. Abujarad, G. Nadim, and A. Omar, "Clutter reduction and detection of landmine objects in ground penetrating radar data using singular value decomposition (SVD)," in *Proc. 3rd Int. Workshop Adv. Ground Penetrating Radar (IWAGPR)*, May 2005, pp. 37–42.
- [25] W. Bi, Y. Zhao, C. An, and S. Hu, "Clutter elimination and random-noise denoising of GPR signals using an SVD method based on the Hankel matrix in the local frequency domain," *Sensors*, vol. 18, no. 10, p. 3422, Oct. 2018.
- [26] W. Xue, Y. Luo, Y. Yang, and Y. Huang, "Noise suppression for GPR data based on SVD of window-length-optimized Hankel matrix," *Sensors*, vol. 19, no. 17, p. 3807, Sep. 2019.
- [27] G. Chen, L. Fu, K. Chen, C. D. Boateng, and S. Ge, "Adaptive ground clutter reduction in ground-penetrating radar data based on principal component analysis," *IEEE Trans. Geosci. Remote Sens.*, vol. 57, no. 6, pp. 3271–3282, Jun. 2019.
- [28] F. Abujarad and A. Omar, "Comparison of independent component analysis (ICA) algorithms for GPR detection of non-metallic land mines," *Proc. SPIE*, vol. 6365, Sep. 2006, Art. no. 636516.
- [29] E. Temlioglu and I. Erer, "Clutter removal in ground-penetrating radar images using morphological component analysis," *IEEE Geosci. Remote Sens. Lett.*, vol. 13, no. 12, pp. 1802–1806, Dec. 2016.
- [30] D. Kumlu and I. Erer, "Clutter removal in GPR images using non-negative matrix factorization," *J. Electromagn. Waves Appl.*, vol. 32, no. 16, pp. 2055–2066, Jun. 2018.
- [31] T. Zhou and D. Tao, "GoDec: Randomized low rank & sparse matrix decomposition in noisy case," in *Proc. 28th Int. Conf. Mach. Learn.*, 2011, pp. 33–40.
- [32] X. Shu, F. Porikli, and N. Ahuja, "Robust orthonormal subspace learning: Efficient recovery of corrupted low-rank matrices," in *Proc. IEEE Conf. Comput. Vis. Pattern Recognit.*, Jun. 2014, pp. 3874–3881.
- [33] D. Kumlu and I. Erer, "GPR clutter reduction by robust orthonormal subspace learning," *IEEE Access*, vol. 8, pp. 74145–74156, Apr. 2020.
- [34] J. Wright, A. Ganesh, S. Rao, and Y. Ma, "Robust principal component analysis: Exact recovery of corrupted low-rank matrices via convex optimization," *Coordinated Sci. Lab., Urbana, IL, USA, Tech. Rep. UILU-ENG-09-2210*, Dec. 2009, p. 243.
- [35] X. Song, D. Xiang, K. Zhou, and Y. Su, "Improving RPCA-based clutter suppression in GPR detection of antipersonnel mines," *IEEE Geosci. Remote Sens. Lett.*, vol. 14, no. 8, pp. 1338–1342, Aug. 2017.
- [36] X. Song, T. Liu, D. Xiang, and Y. Su, "GPR antipersonnel mine detection based on tensor robust principal analysis," *Remote Sens.*, vol. 11, no. 8, p. 984, Apr. 2019.
- [37] D. Kumlu and B. Gündoğdu, "A novel tensor RPCA method for clutter suppression in GPR images," *J. Nav. Sci. Eng.*, vol. 17, no. 1, pp. 27–42, Apr. 2021.
- [38] I. Giannakis, A. Giannopoulos, and A. Yarovsky, "Model-based evaluation of signal-to-clutter ratio for landmine detection using ground-penetrating radar," *IEEE Trans. Geosci. Remote Sens.*, vol. 54, no. 6, pp. 3564–3573, Jun. 2016.
- [39] X. L. Travassos, S. L. Avila, and N. Ida, "Artificial neural networks and machine learning techniques applied to ground penetrating radar: A review," *Appl. Comput. Informat.*, vol. 17, no. 2, pp. 296–308, Jul. 2020.
- [40] D. L. Donoho, "Compressed sensing," *IEEE Trans. Inf. Theory*, vol. 52, no. 4, pp. 1289–1306, Apr. 2006.
- [41] F. Giovanneschi, K. V. Mishra, M. A. Gonzalez-Huici, Y. C. Eldar, and J. H. G. Ender, "Dictionary learning for adaptive GPR landmine classification," *IEEE Trans. Geosci. Remote Sens.*, vol. 57, no. 12, pp. 10036–10055, Dec. 2019.
- [42] J. Hu, Y. Pu, X. Wu, Y. Zhang, and J. Zhou, "Improved DCT-based nonlocal means filter for MR images denoising," *Comput. Math. Method Med.*, vol. 2012, no. 6, Mar. 2012, Art. no. 232685.
- [43] A. Rubel, V. Lukin, and O. Pogrebnyak, "Efficiency of DCT-based denoising techniques applied to texture images," in *Proc. 6th Mex. Conf. Pattern Recognit. (MCP)*, vol. 8495, Jun. 2014, pp. 261–270.
- [44] M. S. El-Mahallawy and M. Hashim, "Material classification of underground utilities from GPR images using DCT-based SVM approach," *IEEE Geosci. Remote Sens. Lett.*, vol. 10, no. 6, pp. 1542–1546, Nov. 2013.
- [45] W. Dong, L. Zhang, R. Lukac, and G. Shi, "Sparse representation based image interpolation with nonlocal autoregressive modeling," *IEEE Trans. Image Process.*, vol. 22, no. 4, pp. 1382–1394, Apr. 2013.
- [46] M. Aharon, M. Elad, and A. Bruckstein, "K-SVD: An algorithm for designing overcomplete dictionaries for sparse representation," *IEEE Trans. Signal Process.*, vol. 54, no. 11, pp. 4311–4322, Nov. 2006.
- [47] M. Elad and M. Aharon, "Image denoising via sparse and redundant representations over learned dictionaries," *IEEE Trans. Image Process.*, vol. 15, no. 12, pp. 3736–3745, Dec. 2006.
- [48] Y. Tang, Y. Shen, A. Jiang, N. Xu, and C. Zhu, "Image denoising via graph regularized K-SVD," in *Proc. IEEE Int. Symp. Circuits Syst. (ISCAS)*, May 2013, pp. 2820–2823.
- [49] T. Chao, W. Zhihui, W. ZeBin, C. Yufeng, and G. Jingping, "Parallel optimization of K-SVD algorithm for image denoising based on spark," in *Proc. IEEE 13th Int. Conf. Signal Process. (ICSP)*, Nov. 2016, pp. 820–825.
- [50] G. Tang, J.-W. Ma, and H.-Z. Yang, "Seismic data denoising based on learning-type overcomplete dictionaries," *Appl. Geophys.*, vol. 9, no. 1, pp. 27–32, Apr. 2012.
- [51] W. Shao, A. Bouzerdoum, and S. L. Phung, "Sparse representation of GPR traces with application to signal classification," *IEEE Trans. Geosci. Remote Sens.*, vol. 51, no. 7, pp. 3922–3930, Jul. 2013.
- [52] Y. Li, A. Cichocki, and S.-I. Amari, "Analysis of sparse representation and blind source separation," *Neural Comput.*, vol. 16, no. 6, pp. 1193–1234, Jun. 2004.
- [53] J. A. Tropp and A. C. Gilbert, "Signal recovery from random measurements via orthogonal matching pursuit," *IEEE Trans. Inf. Theory*, vol. 53, no. 12, pp. 4655–4666, Dec. 2007.
- [54] K. Usman, H. Gunawan, and A. B. Suksmono, "Compressive sensing reconstruction algorithm using L1-norm minimization via L2-norm minimization," *Int. J. Elect. Eng. Inform.*, vol. 10, no. 1, pp. 37–50, Mar. 2018.
- [55] Y. Zhou, H. Zhao, X. Chen, T. Liu, D. Wu, and L. Shang, "Speech denoising based on sparse representation algorithm," in *Proc. 12th Int. Conf. Intell. Comput. (ICIC)*, Aug. 2016, pp. 202–211.
- [56] D. Feng, X. Wang, and X. Wang, "New dynamic stochastic source encoding combined with a minmax-concave total variation regularization strategy for full waveform inversion," *IEEE Trans. Geosci. Remote Sens.*, vol. 58, no. 11, pp. 7753–7771, Nov. 2020.
- [57] Z. Jiang, Z. Zeng, J. Li, F. Liu, and W. Li, "Simulation and analysis of GPR signal based on stochastic media model with an ellipsoidal autocorrelation function," *J. Appl. Geophys.*, vol. 99, pp. 91–97, Dec. 2013.
- [58] D. Feng, X. Wang, B. Zhang, and Z. Ren, "An investigation into the electromagnetic response of porous media with GPR using stochastic processes and FEM of B-spline wavelet on the interval," *J. Appl. Geophys.*, vol. 169, pp. 174–182, Oct. 2019.

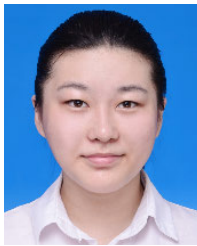


**DESHAN FENG** received the B.S., M.S., and Ph.D. degrees in geophysics from Central South University, Changsha, China, in 2000, 2003, and 2006, respectively.

From 2009 to 2013, he was an Associate Professor with Central South University, where he has been a Professor, since 2014. From March 2013 to March 2014, he was a Visiting Scholar with Rice University, Houston, TX, USA. His research interests include numerical simulation/inversion of

ground penetrating radar and processing of near-surface geophysical data for the nondestructive evaluation of the shallow subsurface.

Dr. Feng is a Reviewer for *Geophysics*, *Computers and Geosciences*, and *Journal of Applied Geophysics*.



**SHUO LIU** was born in Hebei, China, in 1996. She received the B.S. degree in geophysics from the Chengdu University of Technology, Chengdu, China, in 2018. She is currently pursuing the M.S. degree in geological resources and geological engineering with the College of Geosciences and Info-Physics, Central South University, Changsha, China. Her research interests include numerical simulation and signal processing of ground penetrating radar.



**JUN YANG** was born in Fengcheng, Jiangxi, China, in 1980. He received the B.S. degree in exploration of engineering from Central South University, in 2000, and the M.S. degree in project management engineering from the South China University of Technology, in 2007. He is currently the Vice President of the Second Design Institute of Guangzhou Municipal Engineering Design and Research Institute Company Ltd. He has been engaged in geotechnical engineering investigation for a long time.



**XIANGYU WANG** was born in Tianjin, China, in 1993. He received the B.S. and M.S. degrees in geophysics from Central South University, Changsha, China, in 2016 and 2019, respectively. He is currently pursuing the Ph.D. degree in geological resources and geological engineering with the School of Geosciences and Info-Physics, Central South University. His research interests include full-waveform inversion of seismic data and applied deep learning.



**XUN WANG** was born in Xinxiang, Henan, China, in 1990. He received the B.S., M.S., and Ph.D. degrees in geophysics from Central South University, Changsha, China, in 2013, 2016, 2020, respectively.

He is currently a Distinguished Associate Professor with the School of Geosciences and Info-Physics, Central South University. His research interests include simulation of electromagnetic waves and full-waveform inversion of ground penetrating radar data. He is a Reviewer for IEEE ACCESS and IEEE GEOSCIENCE AND REMOTE SENSING LETTERS.

• • •